An Analysis of Heat Transfer and the Impact of Gold and Silver Nanoparticles on Blood Flow within Arterial Stenosis

Tejpal Singh, P. K. Shukla

K. G. K. College Moradabad, MJPRU Bareilly, India

DOI: https://dx.doi.org/10.51584/IJRIAS.2025.1010000050

Received: 07 October 2025; Accepted: 16 October 2025; Published: 03 November 2025

ABSTRACT

The current study's simulation made use of COMSOL Multiphysics' CFD. Blood was used as the basic fluid in this simulation. Blood was considered to be a laminar, unstable, and incompressible Newtonian fluid, and its Newtonian nature is tolerable at high shear rates. The behavior of blood flow was investigated to ascertain the effects of temperature, velocity, and pressure through vascular stenosis. Gold (Au) and silver (Ag) nanoparticles were the two types utilized in this investigation. The mass, momentum, and energy equations were solved using the CFD method.

A fine element size mesh was made using COMSOL. The analysis's conclusions show that the artery's velocity fluctuates over constrained sections, falling both before and after the stenotic zone and being higher in a diseased location. The heat transfer feature's upper and lower boundary temperatures were selected to be 24.85°C and 27.35°C, respectively. The nanoparticles affected the density, specific heat, dynamic viscosity, and thermal conductivity of blood. The use of gold and silver nanoparticles prevented overheating since they both have high thermal conductivity, which is essential for quickly dispersing heat. Nusselt number variations were also calculated, and the results show that the curve decreases inside the stenosis. At t = 0.7 s and 1 s, recirculation occurs right after the stenosed area, and it is possible to infer that the streamlines behave abnormally. These discoveries will have a significant impact on the treatment of stenosed arteries.

Keywords: Newtonian fluid, blood flow, unsteady, CFD, nanoparticles (gold and silver), stenosed, artery.

INTRODUCTION

Nanoparticles aid in the successful treatment of cardiovascular disorders as well as other diagnostic applications. Better treatment approaches are made possible by the physical characteristics of nanoparticles, such as changes to their size, shape, and surface, and these characteristics are primarily responsible for the delivery of nanoparticles into the arteries.

T. Hayat and S. Nadeem [1] investigated how adding copper oxide and silver nanoparticles to water, the base fluid, could improve heat transfer. Single wall carbon nanotubes in blood flow through numerous stenoses were investigated by S. Nadeem and S. Ijaz [2] while taking varying viscosity into account. [3,4] have examined three-dimensional flow models with the addition of nanoparticles and under various impacts. Prandt l magnetoh ydrodynamic nanofluid flow via arterial stenoses was examined by S. Nadeem et al. [5]. One significant and distinct application of nanoparticles is in the contemporary field of medicine. The most influential material in nanoscience and nanomedicine is gold nanoparticles. They are employed as medication transporters, contrast agents, photovoltaic agents, and radioinfection agents. Gold and silver nanoparticles also have a lot of qualities that make them appealing for use in biological diagnosis and treatment. Nanoparticle therapy is still being developed for vascular disorders. In their investigation of blood flow via stenosed vessels, T. Elnaqeeb et al. [6] provided findings for several flow parameters.

They also compared their findings to Cu and TiO_2 models and came to the conclusion that adding gold nanoparticles enhances blood velocity. Numerous researchers [7–10] have focused on the study of vascular disorders using various approaches. Crucial elements of the circulatory system are blood vessels. Transporting vital nutrients and oxygen to the body's active tissues while eliminating waste is the main goal of the circulatory system. Blood flow patterns are crucial to the development and progression of cardiovascular disorders.

Causes	Symptoms	Complications
Rheumatic fever, radiation therapy, calcium accumulation, and birth abnormalities.	palpitations, swelling ankles or feet, chest pain, and trouble walking short distances.	arrhythmias, endocarditis, blood clots, cardiac failure, and stroke.

In recent years, the computational fluid dynamics (CFD) technique has gained utility for problems involving physiological fluxes. CFD's primary goal is to use computational power to numerically simulate fluid motion and heat transport. Using COMSOL, J. Liu et al. [11] investigated numerical solutions to equation-governing issues. The maximum and minimum values for temperature, pressure, and velocity were determined by A. Hussainetal [12] in his study of the heat transfer consequences for laminar and unsteady fluid flow through several elliptic cylinders. This article examines the dynamics of blood flow via a stenosed area. The Newtonian characteristics of blood in big cavities, veins, and arteries led us to infer that blood is a Newtonian fluid. CFD was used to determine the velocity, temperature, and pressure of the blood flow inside the affected area after the law of conservation of mass, momentum, and energy was solved using COMSOL Multiphysics software. In order to find out how hybrid nanoparticles (NPs) can improve blood flow, this article presents the mathematical analysis of adding gold and silver nanoparticles to blood passing through a stenosed area.

MATERIALS AND PROCEDURES

Blood was considered to be an incompressible, unstable Newtonian fluid passing through an artery constriction in this study. Figure 1 depicts a sketch of the arterial stenosis blood flow problem. The coordinate system was chosen so that the blood flow was along the z-axis and r was interpreted as perpendicular to the flow.

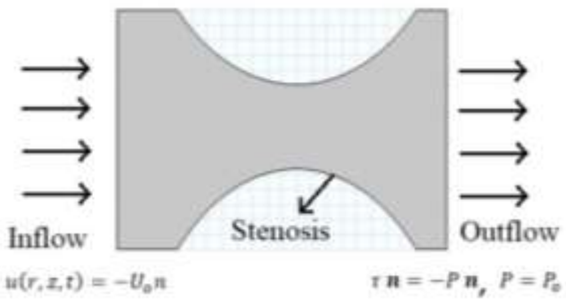

Figure 1. The geometry of arterial stenosis

The two-dimensional artery's coordinate locations were r = 0.1 and z = 0, and its breadth and height were 1.1 and 0.8 meters, respectively. The "add physics" function in COMSOL 5.4 was used to incorporate the physics of laminar blood flow and heat transfer. The entrance and exit locations were chosen, and the velocity was zero at the boundary wall.

19.85 °C was chosen as the reference temperature for the laminar flow and heat transfer. Temperature 1 at the upper boundary was determined to be 24.85 °C, whereas temperature 2 at the lower boundary was 27.35 °C. The initial temperature in the heat transfer was −73.15 °C. Blood's material qualities, or thermophysical qualities, were added. The time-dependent model governing equations, which include the mass, momentum, and heat transfer equations [13, 14], were then included.

2.1 Continuty Equation:

$$\frac{1}{r}\frac{\partial}{\partial r}(ru)+\frac{\partial}{\partial z}(w)=0, \qquad (1)$$

In COMSOL, the equation of continuity that described the blood mass transport was expressed as:

$\nabla . u = 0,$ (2) where u and w are the velocities of the nanofluid denoted in r and z directions, respectively.

2.2 Equation of Motion:

$$\rho_{hnf}\left(\frac{\partial u}{\partial t} + u\frac{\partial u}{\partial r} + w\frac{\partial u}{\partial z}\right) = \frac{\partial p}{\partial r} + \mu_{hnf}\frac{\partial}{\partial z}\left(\frac{\partial w}{\partial r} - \frac{\partial u}{\partial z}\right), \quad (3)$$

$$\rho_{hnf}\left(\frac{\partial w}{\partial t} + u\frac{\partial w}{\partial r} + w\frac{\partial u}{\partial z}\right) = -\frac{\partial p}{\partial z} - \mu_{hnf}\left(\frac{\partial}{\partial r} + \frac{1}{r}\right)\left(\frac{\partial w}{\partial r} - \frac{\partial u}{\partial z}\right). \quad (3)$$

The momentum equation model in COMSOL was displayed as follows:

$$\rho\frac{\partial u}{\partial t} + \rho(u.\nabla)u = \nabla.[-PI + K] + F, \quad (5)$$

$$K = \mu(\nabla u + (\nabla u)^T), \quad (6)$$

whre ρ_{hnf}, μ_{hnf} and P are the density, viscoity and pressure of the nanofluid, respectively.

2.3 Energy Equation:

$$\left(\rho C_p\right)_{hnf}\left(\frac{\partial}{\partial t} + u\frac{\partial}{\partial r} + w\frac{\partial}{\partial z}\right)T = k_{hnf}\left(\frac{\partial^2}{\partial r^2} + \frac{\partial}{r\partial r} + \frac{\partial^2}{\partial z^2}\right)T, \quad (7)$$

In COMSOL, the governing heat transfer equation was

$$d_z\rho C_P\frac{\partial T}{\partial t} + d_z\rho C_p u.\nabla T + \nabla.q = d_z Q + q_0 + d_z Q_P + d_z Q_{vd,} \quad (8)$$

where $q = d_z k\nabla T, q_0 = \frac{q}{A_s\Delta T}, Q_{vd} = \tau.\nabla u, Q_p = \alpha pT\left(\frac{\partial P}{\partial t} + u.\nabla P\right), A_s = 0.8\,m^2, \alpha p = -\frac{1}{\rho}\frac{\partial P}{\partial t}, \tau = -PI + K, d_Z$ is the thickness of the fluid, which is equal to 1 m, Q is the heat source, Q_{vd} is viscous dissipation heat source. ∇T shows the tempetrature gradient, $C_{p,nf}$ shows the heat capacitance of the fluid and k_{nf} is specific heat. The considered initial values are :

$u = w = 0, T = T_0$ and P = 0. (9)

The thermophysical properties of the hybrid nanofluids were defined as follows (15)

$$\left.\begin{aligned}
\rho_{hnf} &= (1-\phi_2)\left((1-\phi_1)\rho_f + \phi_1\rho_{s1}\right) + \phi_2\rho_{s2},\\
\mu_{hnf} &= \frac{\mu_f}{(1-\phi_1)^{2.5}(1-\phi_2)^{2.5}},\\
\left(\rho C_p\right)_{hnf} &= (1-\phi_2)\left((1-\phi_1)\left(\rho C_p\right)_f + \phi_1\left(\rho C_p\right)_{s1}\right) + \phi_2\left(\rho C_p\right)_{s2},\\
\frac{k_{hnf}}{k_f} &= \frac{k_{s_1}+2k_f-2\phi_1\left(k_f-k_{s_1}\right)}{k_{s_1}+2k_f+\phi_1\left(k_f-k_{s_1}\right)} \times \frac{k_{s_2}+2k_{nf}-2\phi_2\left(k_{nf}-k_{s_2}\right)}{k_{s_2}+2k_{nf}+\phi_2\left(k_{nf}-k_{s_2}\right)}.
\end{aligned}\right\} \quad (10$$

2.4. Boundary Conditions:

Inlet, outflow, wall, and thermal insulation were all part of the boundary conditions.

The Inlet: At the artery's inlet, the velocity, or blood flow rate, was simulated. The area of the inflow cross-section and the velocity at the intake could be used to regulate the blood volume. The model's inlet definition is depicted in Figure 2.

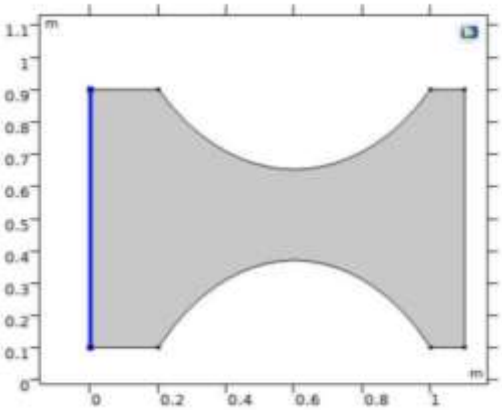

Figure 2. The geometry of the inlet.

The inlet boundary condition was:

$$u(r, z, t) = -U_0 n, \qquad (11)$$

where U_o is the normal inflow velocity, which is equal to 0.5.

The Outlet: To give the simulation a more genuine feel, we introduced the blood flow model's pressure at the outlet. The exit, where the blood poured out, is shown in Figure 3. It was located on the other side of the entrance.

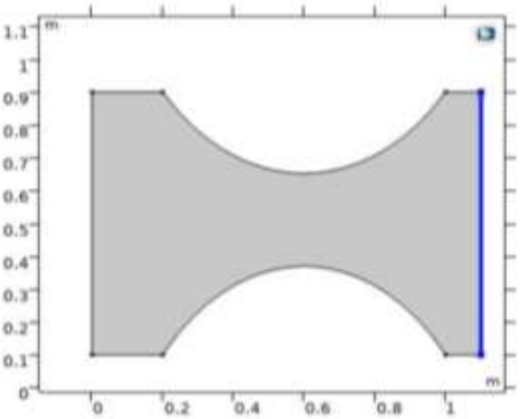

Figure 3. The geometry of the outlet.

In COMSOL, the equation at the outlet was given as :

$$\tau\, n = -P\, n, where\ P = P_0, \qquad (12)$$

where $n = (n_r, n_z)$ is the pointing normal outflow velocity and the absolute pressure is $P_0 = 0$ Pa.

At the Wall : Because blood is viscous, it adheres to the wall and cannot pass through it. Consequently, the boundary conditions at the wall were :

$$u = 0, w = 0. \qquad (13)$$

and no slip condition was considered. Figure 4 represent the wall of arterial stenosis.

ISSN No. 2454-6194 | DOI: 10.51584/IJRIAS | Volume X Issue X October 2025

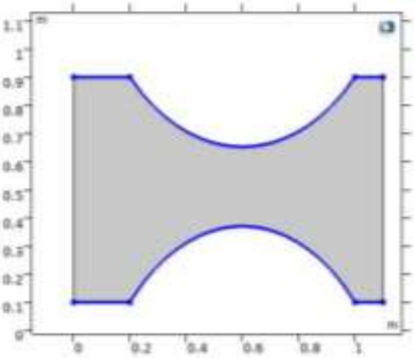

Figure 4. The wall of arterial stenosis.

Thermal Insulation:

The insulated boundaries in the COMSOL heat transfer feature are shown in Figure 5.

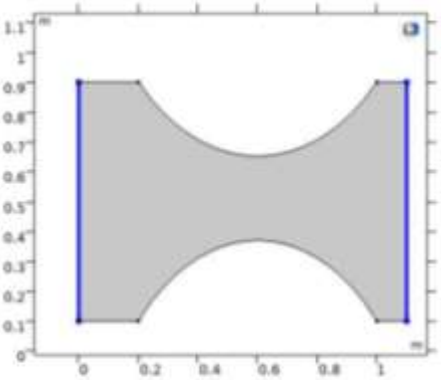

Figure 5. The thermal insulated boundaries of the problem.

The thermal insulation equation used in COMSOL was :

$$-n.q = 0 \qquad (14)$$

2.5. Computational Mesh

One of the key components of computational fluid dynamics is mesh. The mesh quality can be used to determine the accuracy of the solution and the pace of convergence. Mesh is automatically created by COMSOL's "physics controlled mesh" function. Meshes with finer element sizes perform better and yield more accurate results than those with larger elements. The "normal" and "fine" element size meshes are depicted in Figures 6 and 7. It was found that the mesh was less refined when it was far from the stenosis and more refined in the stenosed area.

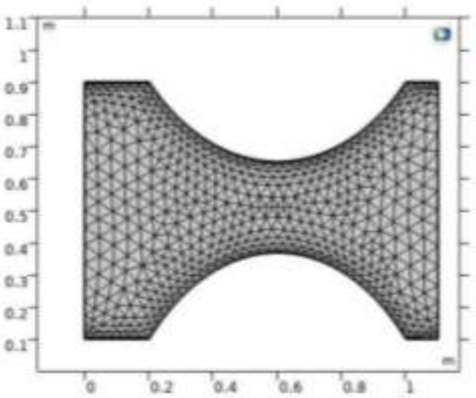

Figure 6. Normal element size mesh

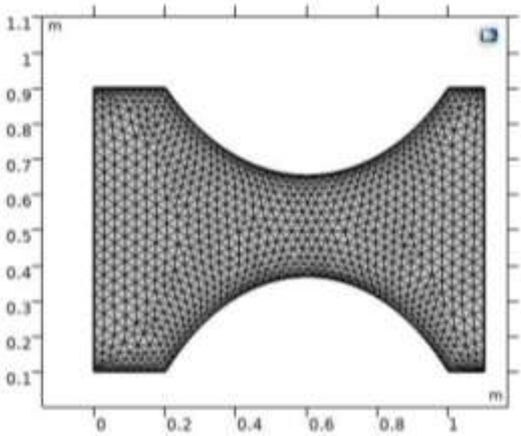

Figure-7. Find element size mesh.

VALIDATION

The results produced by adding a hybrid nanoparticle were compared to those of [15] in order to assess the problem's correctness. The starting velocities of 0.1 and 0.05 were chosen. We used a starting velocity of 0.5 in our simulation. The findings of our simulation show that adding nanoparticles enhanced the velocity outcome, even if the other circumstances remained the same. There is good agreement between the current results and [15].

RESULTS

An important and difficult subject is the mathematical analysis of blood flow in the arteries. Arterial stenosis, the contraction and hardening of blood channel walls, is the most prevalent illness in the arterial system. When hybrid nanoparticles are added to arteries with stenosis, a mathematical model to determine the blood's velocity, temperature, and pressure was examined. The simulation findings changed when hybrid nanoparticles were included because they altered the physical characteristics of blood, including its density, specific heat, dynamic viscosity, and thermal conductivity. Nusselt number variation was examined in order to observe the heat transport phenomenon. The problem's two-dimensional drawing is displayed in Figure 1. The blood flow's entrance point is shown in Figure 2, and this boundary condition also determined the fluid's velocity. The fluid flowed out of the outlet point, which is depicted in Figure 3. The problem's wall and thermal insulation borders are depicted in Figures 4 and 5, respectively. The boundary conditions for thermal insulation suggested that the simulation's heat source had no effect on the circumstances. We examined the effects of normal and fine element size meshes on the outcomes, which are displayed in Figures 6 and 7. There were 1529 elements in total, with the mesh vertices of the normal element size being 948, the total triangles being 1315, the quad entities being 214, the highest element size being 0.0737, and the minimum being 3.3×10^{-4}. The resolution of the narrow region was 1, the minimum element size was 8×10^{-4}, the maximum element size was 0.028, the total number of elements was 1981, the mesh vertices of the fine element size were 1195, the total triangles were 1747, the quad entities were 234, and the vertex elements were 8. The temporal variations for velocity, pressure, temperature, isothermal contours, and streamlines for t = 0.1 s, 0.7 s, and 1 s are shown in Figures 8–21. Figures 8–10 illustrate the velocity profile's effects. At t = 0.1 s, the velocity in Figure 8 is 1.59 m/s. The top speed in Figure 9 is 1.57 m/s at 0.7 s. The top speed in Figure 10 is 1.58 m/s at 1 s. The findings indicate that t = 0.1 s, or 1.59 m/s, was the maximum velocity. As can be observed, the inlet's flow pattern was smooth. Additionally, compared to both before and after the stenosis, the sick region had a higher velocity.This was expected as the narrow zone should have a higher velocity according to the results of Bernoulli's equation. The temperature profiles for heat transport are displayed in Figures 11–13. While the temperature fluctuated over time, the upper and lower temperature limits stayed constant at 26.85 0C and -73.15 0C, respectively. The findings demonstrate that the heat transfer ratio was successfully increased by the use of nanoparticles.The pressure profiles are displayed in Figures 14–16. At t = 1 s, the pressure reached its highest and minimum values. The pressure was at its lowest toward the end of the stenosis, while it was at its highest right before the stenosed area. The isothermal contours for the temperature profiles are displayed in Figures 17–19. The isothermal contours' minimum contours were discovered at t = 0.1 s, while their maximum range stayed constant. The contour pattern dispersed and moved out of the confined area. The streamlines that recirculated following the stenosis are shown in Figures 20–22. The Nusselt number (Nu) was used to analyze the overall heat transfer. Figure 23 shows how the Nuav number changes over time in the current problem. It is evident that as the fluid flow reached the stenosis borders, the Nusselt number decreased, and that the average Nusselt number rose before and after that point at different periods. The current model is validated in Figure 24.

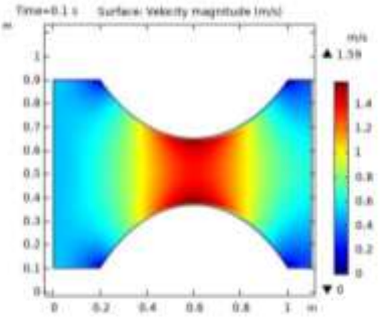

Figure 8. The velocity profile at t = 0.1 s.

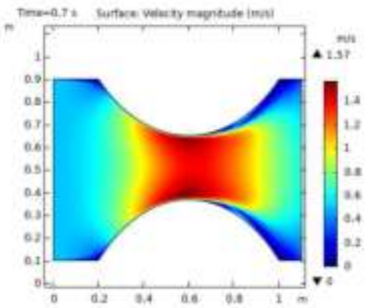

Figure 9. The velocity profile at t = 0.7 s.

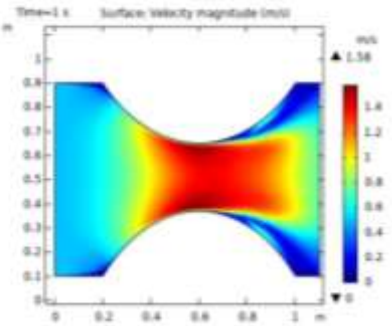

Figure 10. The velocity profile at t = 1 s.

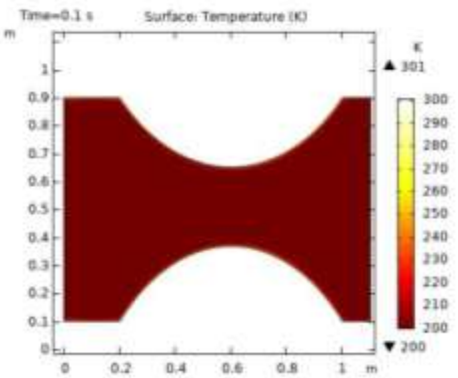

Figure. 11. The temperature profile at t = 0.1 s.

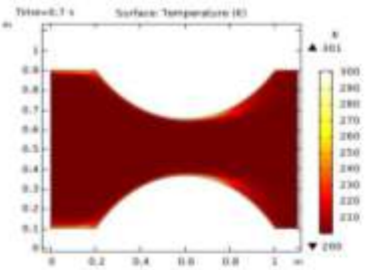

Figure. 12. The temperature profile at t = 0.7 s.

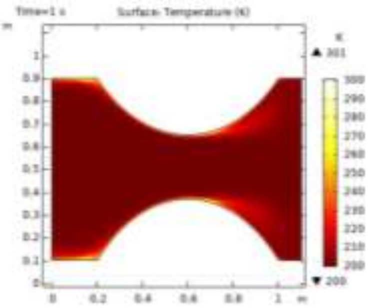

Figure. 13. The temperature profile at t = 1 s.

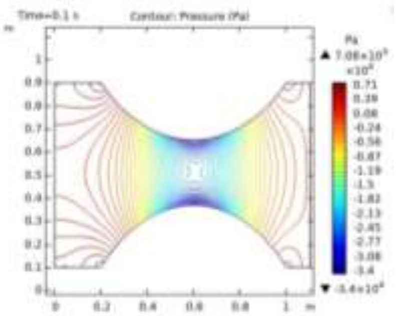

Figure 14. The pressure profile at t = 0.1 s.

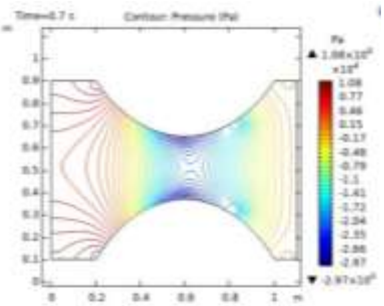

Figure 15. The pressure profile at t = 0.7 s.

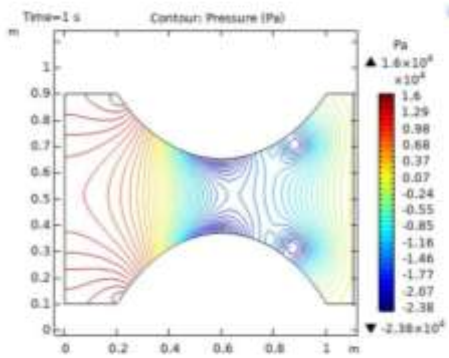

Figure 16. The pressure profile at t = 1 s.

ISSN No. 2454-6194 | DOI: 10.51584/IJRIAS | Volume X Issue X October 2025

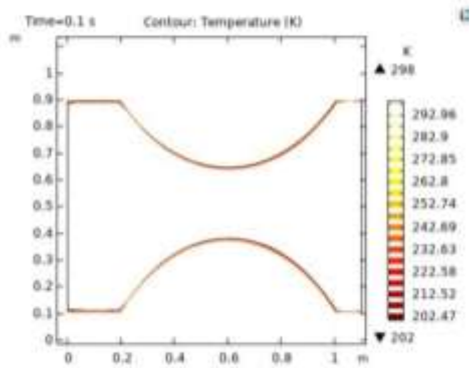

Figure 17. The isothermal contour profile at t = 0.1 s.

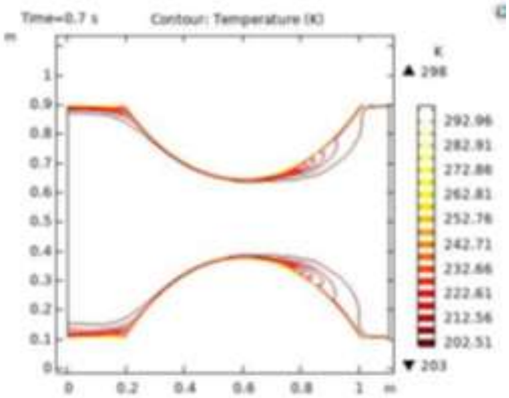

Figure 18. The isothermal contour profile at t = 0.7 s.

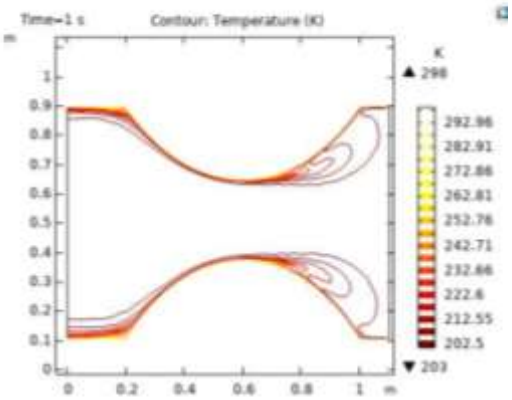

Figure 19. The isothermal contour profile at t = 1 s.

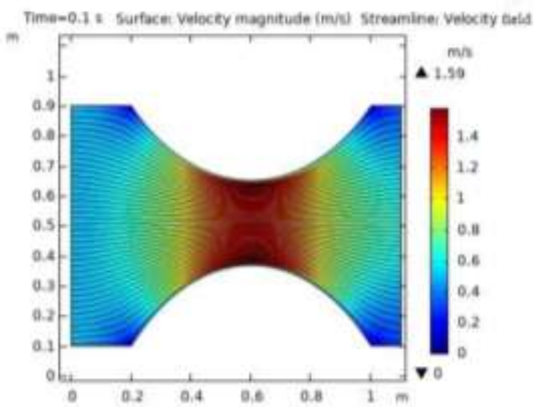

Figure 20. The streamlines at t = 0.1 s.

ISSN No. 2454-6194 | DOI: 10.51584/IJRIAS | Volume X Issue X October 2025

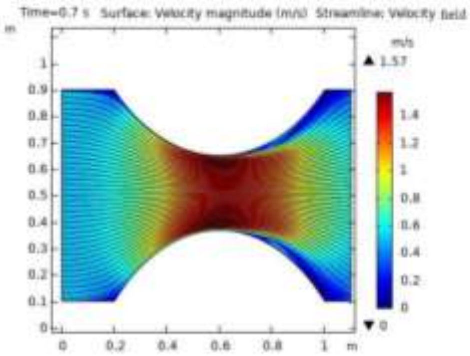

Figure 21. The streamlines at t = 0.7 s.

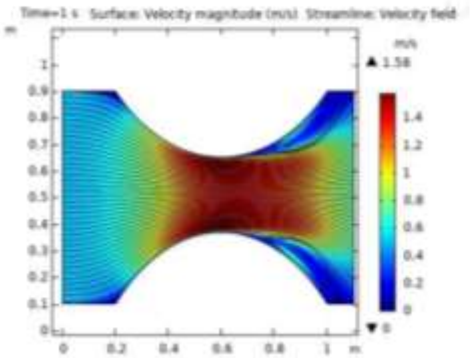

Figure 22. The streamlines at t = 1 s.

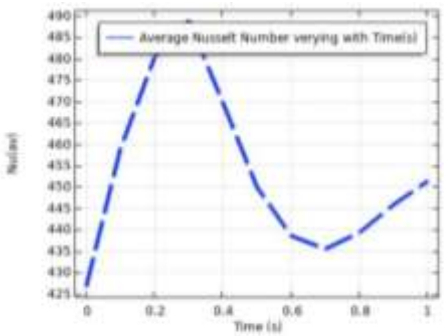

Figure 23. The Nusselt number variation with time.

The calculated mesh element size and area in m_2 for the normal and fine settings are shown in Table 1. For improved performance and more accurate results, we utilized the fine element size mesh. The mesh statistics for the mesh elements, mesh area, mesh quality, total number of triangular and quadrilateral entities, and total number of elements are described in Table 2. The stenosed artery's mesh size, including its maximum and minimum mesh element sizes, narrow region resolution, maximum element growth rate, geometric entity level, and curvature factor, is displayed in Table 3.

A key component of the simulation is the mesh pieces' quality and resolution. The dynamic viscosity, thermal conductivity, heat capacity, and density of the blood were all impacted by the characteristics of the blood base fluid and the gold and silver nanoparticles used to determine the solution in Table 4.

Table 1. The mesh elements computed using COMSOL.

	Elements	Element Size	Mesh Area
	Mesh 1	Normal	0.5949 m^2
Present study	Mesh 2	Fine	0.5948 m^2

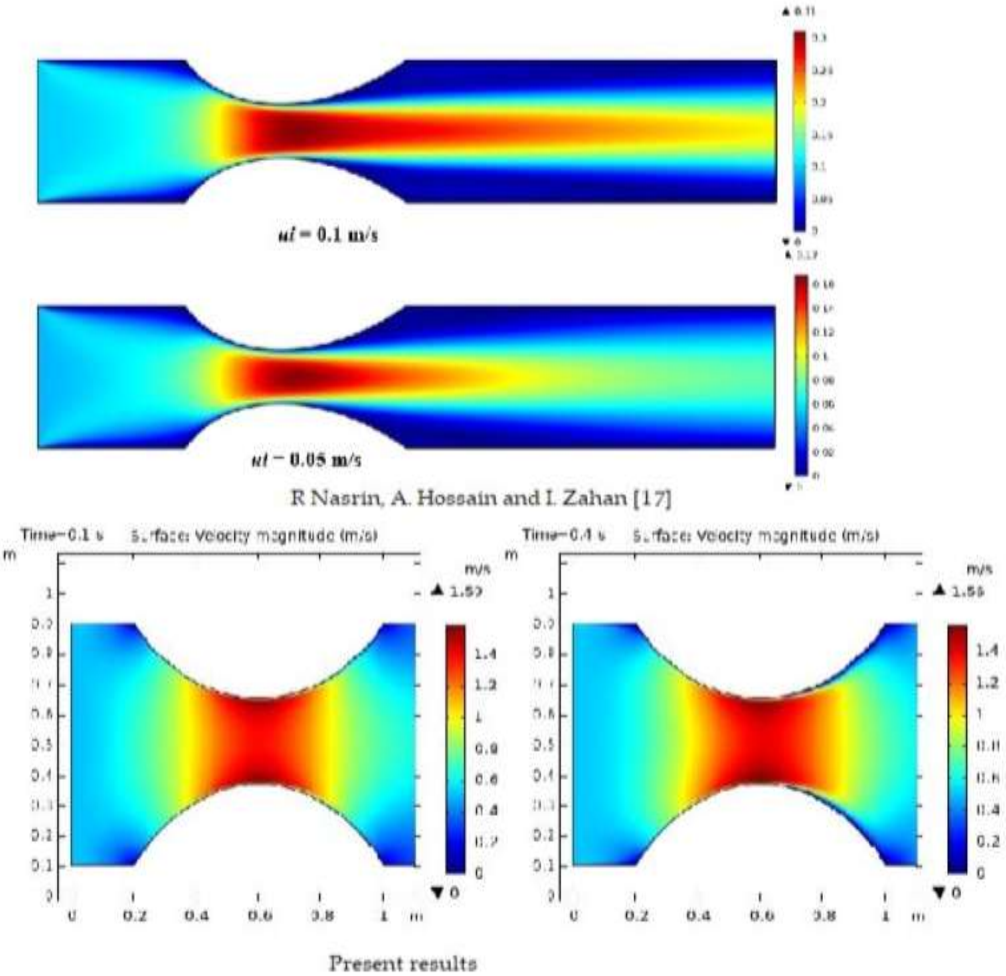

Figure 24. The validation figures with [17] and our obtained results.

Table 2. A description of the mesh statistics.

Property	**Value**
Mesh vertices	1195
Edge elements	173
Quadrilateral entities	234
Triangles	1747
Vertex elements	8
Average element quality	0.8291
Minimum element quality	0.3539
Mesh area	0.5948 m^2
Total no. of elements	1981
Ratio area of element	0.06767

Table 3. A description of the mesh sizes.

Property	**Value**
Maximum element growth rate	1.13

Maximum element size	0.028
Minimum element size	8 x 10^{-4}
Curvature factor	0.3
Resolution of narrow region	1
Geometric entity level	Entire geometry

Table 4. The thermophysical properties of the blood fluid and the silver and gold nanoparticles [16].

Property	**Variable**	**Blood**	**Gold**	**Silver**	**Unit**
Dynamic viscosity	μ	0.003	0.00464	0.005	Pa. s
Heat capacity	C_p	3746	129	235	J/(kg. K)
Thermal conductiry	K	0.52	310	429	W/(m. K)
Density	ρ	1063	19,300	10,500	Kg/m^2

CONCLUSIONS

We looked into how utilizing hybrid nanoparticles affected the flow of blood through an artery that was damaged. This study's primary goal was to report the CFD results for the pressure, temperature, and velocity across the artery's narrow section. The results show that the inclusion of silver and gold nanoparticles inhibited the maximum velocity and prevented overheating. Hemodynamics could be better understood by using our simulations. Among the primary findings were:

- The laminar flow investigation demonstrated that arterial plaque causes variations in the blood flow velocity throughout the model.
- The maximum velocity of the blood flow was 1.59 m/s at t = 0.1 s;
- The isothermal contours clearly showed the results on colored surfaces at t = 0.1, 0.7, and 1 s;
- The temperature and Nusselt number curves varied for slight variations of time; • The pressure profiles also showed clear patterns near the stenosed region;
- The streamlines displayed abnormal behavior near the stenosis area and that recirculation occurred as the intensity of the stenosis increased; the flow was normal when nanoparticles were added;
- We can further study the physical characteristics, such as skin friction coefficient, and also analyze the problem using radiation and magnetohydrodynamic effects to understand the causes of stenosis, which may aid in the treatment of arterial stenosis.

REFERENCES

1. Hayat, T.; Nadeem, S. Heat transfer enhancement with Ag-CuO/water hybrid nanofluid. Results Phys. 2017, 7, 2317–2324. [CrossRef]
2. Nadeem, S.; Ijaz, S. Single wall carbon nanotube (SWCNT) examination on blood flow through a multiple stenosed artery with variable nanofluid viscosity. AIP Adv. 2015, 5, 107217. [CrossRef]
3. Ghadikolaei, S.; Gholinia, M. Terrific effect of H2 on 3D free convection MHD flow of C2H6O2H2O hybrid base fluid to dissolve Cu nanoparticles in a porous space considering the thermal radiation and nanoparticle shapes effects. Int. J. Hydrog. Energy 2019, 44, 17072–17083. [CrossRef]

4. Ghadikolaei, S.; Gholinia, M.; Hoseini, M.; Ganji, D. Natural convection MHD flow due to MoS2-Ag nanoparticles suspended in C2H6O2H2O hybrid base fluid with thermal radiation. J. Taiwan Inst. Chem. Eng. 2019, 97, 12–23. [CrossRef]
5. Ijaz, S.; Sadiq, M.A. Inspiration of Induced Magnetic Field on a Blood Flow of Prandtl Nanofluid Model with Stenosis. Curr. Nanosci. 2014, 10, 753–765. [CrossRef]
6. Elnaqeeb, T.; Shah, N.A.; Mekheimer, K. Hemodynamic Characteristics of Gold Nanoparticle Blood Flow Through a Tapered Stenosed Vessel with Variable Nanofluid Viscosity. BioNanoScience 2019, 9, 245–255. [CrossRef]
7. Nadeem, S.; Ijaz, S.; Akbar, N.S. Nanoparticle analysis for blood flow of Prandtl fluid model with stenosis. Int. Nano Lett. 2013, 3, 35. [CrossRef]
8. Ahmed, A.; Nadeem, S. Biomathematical study of time-dependent flow of a Carreau nanofluid through inclined catheterized arteries with overlapping stenosis. J. Cent. South Univ. 2017, 24, 2725–2744. [CrossRef]
9. Ijaz, S.; Nadeem, S. Examination of nanoparticles as a drug carrier on blood flow through catheterized composite stenosed artery with permeable walls. Comput. Methods Programs Biomed. 2016, 1339, 83–94. [CrossRef] [PubMed]
10. Akhtar, S.; McCash, L.B.; Nadeem, S.; Saleem, S.; Issakhov, A. Mechanics of non-Newtonian blood flow in an artery having multiple stenosis and electroosmotic effects. Sci. Prog. 2021, 104, 1–15. [CrossRef] [PubMed]
11. Liu, J.; Wang, G.; Zhang, L.; Shi, Y.; Zhang, H.; Yao, S.-C. Numerical simulation of single bubble boiling behavior. Propuls. Power Res. 2017, 6, 117–125. [CrossRef]
12. Hussain, A.; Hassan, A.; Al Mdallal, Q.; Ahmad, H.; Rehman, A.; Altanji, M.; Arshad, M. Heat transportation enrichment and elliptic cylindrical solution of time-dependent flow. Case Stud. Therm. Eng. 2021, 27, 101248. [CrossRef]
13. Choudhari, P.; Panse, M. Finite Element Modeling and Simulation of Arteries in the Human Arm to Study the Aortic Pulse Wave Propagation. Procedia Comput. Sci. 2016, 93, 721–727. [CrossRef]
14. Durantes, R.; Moon, J.; Pacheco, R.; Pacheco-Vega, A. Numerical Modeling of Single-Phase Fluid-Flow in Wavy Micro-Channels. In White Papers and Application Notes; California State University-Los Angeles: Los Angeles, CA, USA, 2020. Available online: https://www.comsol.com/paper/numerical-modeling-of-single-phase-fluid-flow-in-wavy-micro-channels-9371(accessedon 28 November 2021).
15. Ghadikolaei, S.; Gholinia, M. 3D mixed convection MHD flow of GO-MoS2 hybrid nanoparticles in H2O-(CH2OH)2 hybrid base fluid under the effect of H2 bond. Int. Commun. Heat Mass Transf. 2020, 110, 104371. [CrossRef]
16. Tripathi, J.; Vasu, B.; Bég, O.A.; Gorla, R.S.R. Unsteady hybrid nanoparticle-mediated magneto-hemodynamics and heat transfer through an overlapped stenotic artery: Biomedical drug delivery simulation. Proc. Inst. Mech. Eng. Part H J. Eng. Med. 2021, 235, 1175–1196. [CrossRef] [PubMed]
17. Nasrin, R.; Hossain, A.; Zahan, I. Blood flow analysis inside a stenotic artery using Power-Law fluid model. RDMS 2020, 13, 1–10. [CrossRef]